

CORROSION AND INHIBITION STUDIES ON AISI 316 WITH AISI 410 FIBER LASER WELDED JOINTS

Sathish Rengarajan¹, A. Sathish Kumar^{2*} and R. Ashok Kumar³

¹Department of Mechanical Engineering, St. Joseph's College of Engineering, Chennai-119, Tamil Nadu, India

²Department of Mechanical Engineering, St. Joseph's Institute of Technology, Chennai-119, Tamil Nadu, India

³SRM Madurai College for Engineering and Technology, Madurai, Tamil Nadu, India

(Received September 25, 2023; Revised January 30, 2024; Accepted January 31, 2024)

ABSTRACT. In this investigation, the corrosion study was conducted on fiber laser welded joints of AISI 410 and 316L stainless steel plates using hydrochloric acid, basic, and salt medium, behavior in three different pH. The effects of three different corrosive atmospheres were examined using the weight loss method. The test sample which was exposed to 1 N hydrochloric acid medium for 48 Hours resulted in 0.006 g of weight loss. The maximum amount of corrosion was found in the acidic medium whereas the least was observed in the salt medium. The effectiveness of three distinct derivatives of 1H-indole-2,3-dione, each replaced with hydroxyl groups in various positions, in inhibiting corrosion. Among the three derivatives examined, it was observed that those with ortho and para hydroxyl group substitutions exhibited superior inhibitory properties.

KEY WORDS: Fiber laser welding, Traverse speed, Corrosion study, Isatin Schiff base, Inhibitors

INTRODUCTION

The necessity for the joining of dissimilar materials has emerged as an unavoidable requirement in the engineering sector in recent years [1, 2]. The utilization of welded joints composed of dissimilar materials is becoming more prevalent across numerous industries, such as automotive, chemical, and spacecraft. These joints allow a great deal of flexibility and are increasingly being used in these industries. It is difficult to weld dissimilar materials by conventional methods without any defects due to high heat affected zone, thermal distortion, wrappage, and does not occur deep penetration, controlling the heat generation [3]. In this situation, laser welding has proven to be one of the effective ways to combine dissimilar types of materials and certain problems such as changes in mechanical characteristics, the emergence of intermetallic brittle phases, and thermal distortion need to be resolved in dissimilar joining [4]. The most crucial factor in determining the weld quality among these is the existence of intermetallic brittle phases. Stress corrosion cracking, hydrogen embrittlement, ductility dip cracking, and carbon migration occur in steel and nickel alloys due to mechanical and physical qualities, not in chemical composition. Destructive secondary phase production, carbon diffusion issues, δ -ferrite phase in the fusion zone, and residual stresses must be addressed for weld quality. Every aspect that can induce intermetallic brittle phases indeed needs to be researched and evaluated. Fiber laser welding [FLW] is a method that involves rapid heating and cooling and has very little distortion, great accuracy, and flexibility. It also can precisely adjust energy input [5-9]. The majority of researchers joined dissimilar materials employing fiber laser welding to improve the quality of the weld.

Stainless steels are becoming desirable materials for use in a variety of industrial applications, including the automotive, aerospace, biomedical, steam generating, chemical, and transportation

*Corresponding author. E-mail: sksat29@gmail.com

This work is licensed under the Creative Commons Attribution 4.0 International License

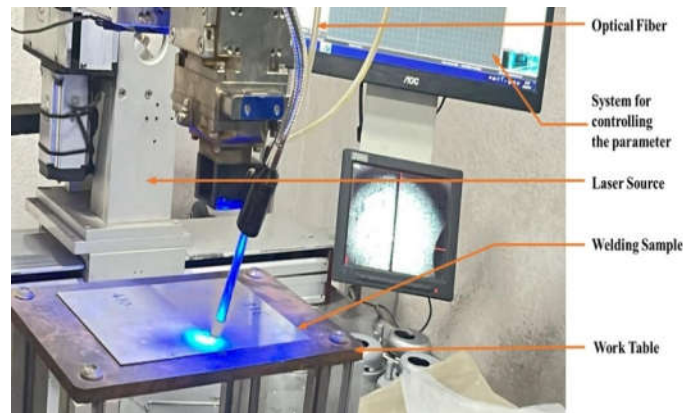
industries [10, 11]. According to a general definition, corrosion is the electrochemical or chemical deterioration of a substance that may or may not be accompanied by mechanical stress. A thorough understanding of how to create a high-quality weld joint will be given by a study on the corrosion of dissimilar welded joints. Verma *et al.* [12] investigated the corrosion failure of welded joints of chromium series stainless steel and 316L dissimilar steel in a modified challenging atmosphere. They suggested that the welding seam has less corrosion resistance than base metal because it contains alloying components with low synergy. Zhang *et al.* [13] carried out a corrosion investigation on dissimilar welded joints made of high-strength steel and austenitic stainless steel. According to research, austenite in the mixed zone has more corrosion resistance than martensite in the weld zone. The welding of stainless steel causes a thermal cycle of rapid heating and cooling, which results in a non-uniform microstructure, heterogeneous chemical composition, mismatched stress, and lattice defects. This alters the corrosion resistance and mechanical properties of the weld metal [WM] and its surrounding areas [14-17]. Corrosion will always have an impact, but its extent and severity can be reduced. However, from an application standpoint, preventing corrosion is a crucial concern, and it has been stated that using inhibitors that serve as barriers is necessary to lessen the aggressive nature of the surroundings [18]. Due to their financial implications, the research of corrosion inhibitors has become a significant industrial and academic subject. To provide essential features of metal corrosion processes and corrosion inhibition across scientific studies, researchers have been tackling this topic in a variety of methods [19]. Behpour *et al.* [20] stated that the stainless steel is corroded by the hydrochloric acid solution. As a result, various inhibitors are employed and injected into solutions to primarily lower the corrosion rate to a safe level.

Reinforced TiN (titanium nitride) and hBN (hexagonal boron nitride) particles on Mg composites and studied the corrosion behaviour at varying ageing temperature particles significantly improved the corrosion resistance of both composites and hybrid composites during the tribo-corrosion test [21]. The influence of NaCl in magnesium metal matrix composites reinforced with ZnO, MnO, and TiO₂, these inclusive enhanced the corrosion behaviour of the composites [22]. The electrochemical studies revealed that Z91D/TiO₂ nanocomposite showed minimal OCP drop (-0.7 to -1.0 V) and COF (0.10) at 2.5% NaCl concentration due to a thick oxide layer that shielded the surface from wear and Cl⁻ during the tribo-corrosion test [23]. To our author's knowledge and from the literature it is revealed that the works are concentrated-based conventional welding such as MIG, TIG welding process, and the corrosion behaviour of the weld joint only. Few works of literature are available to protect the weld joints from corrosion attacks. Keeping the above problems this current work focuses on the investigation of the corrosion behaviour of the AISI 410 and AISI 316 fiber welded samples by varying the process parameters such as frequency, power, and traverse speed. The weight loss method was employed for the AISI 316 stainless steel and AISI 410 stainless steel welded samples. They are immersed in different corrosive mediums such as HCl [acid], NaOH [base], and NaCl [salt] solution media. The three inhibitors were prepared using isatin with ortho, meta, and para-substituted anisidine [24]. These three inhibitors are studied by proton nuclear magnetic resonance [¹H-NMR] spectroscopy after being synthesized by a simple condensation procedure. Inhibitors were employed for novel corrosion control research on laser-welded samples after the confirmation [25].

EXPERIMENTAL

In this process, fiber laser welding was used to weld SS316 and SS410 Stainless plates. The fiber laser welding setup is shown in Figure 1. The chemical composition of the AISI316 and AISI410 is shown in the Table 1. Nine plates of dimension of [100 × 150 × 2 mm], were used for this study. The process parameters used in the welding process are laser power [1000-1980 W], frequency [4000-5000 Hz], transverse speed [3-9 mm/s], and using the Taguchi method shown in Table 2. The weld parameters were chosen to produce welds of high quality based on the literature and

with trial-and-error method. It involves orthogonal array to reduce the variation in a process to get optimum output, it also investigates that parameters affect the mean and variance of a process performance characteristics. The prepared samples were cut for the corrosion test using the wire-cut electrode discharge machine [WEDM] and subjected to a tensile testing machine shown in Figure 1(b). The corrosion inhibition study and the corrosive behavior of the weldment were investigated. Various corrosive media used in weight loss methods are NaOH, HCl and NaCl. Chemicals such as Isatin and three anisidines were purchased from Sigma Aldrich, India, and TCI chemicals. In addition, a Corrosion inhibition study was conducted using three isatin Schiff base derivatives.



(a)



(b)

Figure 1. (a) Fiber laser welding setup. (b) Specimen under tensile testing.

Table 1. Chemical composition [at. %] of SS410 and SS316.

Materials	C	Mn	S	P	Si	Cr	Ni	Fe
AISI 316	0.09	1.0	0.03	0.04	1.0	12.5	0.75	Bal.
Materials	C	Mn	Si	Cr	Ni		Fe	
AISI 410	<0.13	2.02	1.48	17.06– 9.28	9.44- 13.28		Bal.	

Table 2. Taguchi L9 orthogonal array.

S. No	Frequency (Hz)	Power (W)	Traverse speed (mm/min)	Tensile strength MPa
1	4000	1000	6	417.8
2	4000	1490	9	387.3
3	4000	1980	3	397.3
4	4500	1000	6	358.9
5	4500	1490	9	421.3
6	4500	1980	3	475.4
7	5000	1000	6	134.5
8	5000	1490	9	360.2
9	5000	1980	3	409.4

Corrosive medium preparation

The rate of corrosion in the welded joint of AISI 316 and AISI 410 was conducted by weight loss method in three artificial corrosive mediums. After welding, the samples were prepared to the required dimensions [$0.3 \times 3 \times 2 \text{ cm}^3$] for corrosion study. 83 mL of hydrochloric acid was dissolved in 1 liter of water and used for the corrosion trials for the acid medium. Similarly, for alkali medium preparation, 40 g of sodium hydroxide was dissolved in 1 liter of water. To prepare a salt medium, 1 M sodium chloride was prepared with 58.5 g of commercial crystal salt dissolved in 1 liter of water. The prepared 1 M solutions were used for the corrosion study. The hydrogen ions concentration present in each solution was measured using a deep vision pH meter and glass electrode.

Weight loss study in salt, acid and alkali medium

A total of 27 samples (9 samples \times 3) media were prepared and in each corrosive medium, nine samples were kept in three solutions for a total of 48 hours. The corrosion studies were conducted using 1 M HCl [acidic medium], 1 M NaOH solution [basic medium], and 1 M NaCl solution [salt medium] in both the presence and absence of inhibitors. Each sample was cleaned with water and dried at 80 °C for 1 hour. The samples were weighed after drying and placed in prepared corrosive media such as 1 M NaCl, 1 M HCl, and basic 1 M NaOH solutions.

Preparation of Schiff base inhibitors

In a 500 mL three-neck round bottom flask, 3 g of isatin [10 mmol] was treated with 100 mL of ethanol and 1.5 mL of acetic acid. The mixture was then mixed at room temperature for 30 min. Following stirring, 2.5 g of O-anisidine was added to 70 mL of ethanol dropwise over 30 min. The mixture was then swirled once more for 15 min at room temperature. As per the recommended procedure, the entire reaction mixture was refluxed for 2 hours [26]. TLC was used to monitor the reaction's development while employing 60:40 ethyl acetate and hexane with a drop of acetic acid. Following filtration, the product was recrystallized from ethanol. Similarly, the remaining derivatives were derived and the structures are presented in Figure 2.

¹H-NMR chemical shifts of isatin derivatives

The derived compounds are directly characterized by proton NMR [¹H-NMR] for structural confirmation.

¹H NMR [500 MHz, DMSO-d₆] ortho-is-sb C₁₅H₁₂N₂O₂ δ 10.1 [s, 1H], 8.5 [J = 7.0, 1.3 Hz, 1H], 8.31 [J = 7.5, 1.3 Hz, 1H], 7.76 [J = 7.4, 1.3 Hz, 1H], 7.66 [J = 7.9, 1.4 Hz, 1H], 7.45 [J =

7.2, 1.6 Hz, 1H], 7.26 – 7.20 [1H], 7.09 [J = 7.1, 1.2 Hz, 1H], 6.93 [J = 7.3, 1.3 Hz, 1H], 4.09 [J = 6.8 Hz, 3H].

¹H NMR [500 MHz, DMSO-d₆] meta-is-sb C₁₅H₁₂N₂O₂ δ 10.1 [s, 1H], 8.5 [J = 7.0, 1.3 Hz, 1H], 8.31 [J = 7.5, 1.3 Hz, 1H], 7.76 [J = 7.4, 1.3 Hz, 1H], 7.45 [J = 7.2, 1.6 Hz, 1H], 7.28 [J = 7.6 Hz, 1H], 6.83 [J = 7.3, 1.8, 1.0 Hz, 1H], 6.73 [J = 1.9 Hz, 1H], 6.40 [J = 7.8, 1.8, 1.0 Hz, 1H], 4.09 [J = 6.8 Hz, 3H].

¹H NMR [500 MHz, DMSO-d₆] para-is-sb C₁₅H₁₂N₂O₂ δ 10.1 [s, 1H], 8.5 [J = 7.0, 1.3 Hz, 1H], 8.31 [J = 7.5, 1.3 Hz, 1H], 7.76 [J = 7.4, 1.3 Hz, 1H], 7.45 [J = 7.2, 1.6 Hz, 1H], 7.12 – 7.06 [2H], 6.99 – 6.93 [2H], 4.09 [J = 6.8 Hz, 3H].



Figure 2. Structure and immersion of prepared isatin Schiff base derivatives.

Inhibition study

To understand the requirement of inhibitors for welded samples in operating conditions, this work initiated the organic imines for the inhibitor study on fiber laser welded joints. When comparing the metal surface, joints are corroded fast. The corrosion study extended using prepared three derivatives and was subjected to the corrosion study, as shown in Figure 3.



Figure 3. Samples are subjected to three derivatives.

Novel applications in corrosion control of ortho, meta, and para anisidine with isatin condensed imine molecules such as ortho-is-sb [Comp. 1], meta-is-sb [Comp. 2], and para-is-sb [Comp. 3] were carried out for inhibition study. Based on the molecular structure, the position of the methoxyl group concerning the nitrogen atom can be studied clearly. Eugene Uwiringiyimana *et al.* [27] correlated the inhibition efficiency with corrosion inhibitor concentrations and the effect of temperature on stainless steel.

A total of 9 samples were taken to conduct an inhibition study using three derivatives. Out of nine samples, three samples were used to investigate each compound corrosion control tendency in an acid medium. Ahmed *et al.* [28] used a unique organic corrosion inhibitor that was tested in a 1 M hydrochloric acid solution for its ability to prevent corrosion in mild steel. This demonstrates that such inhibitors help slow down and reduce the corrosion process that affects mild steel when exposed to a solution of hydrochloric acid because they give the metal an organic inhibitor that can be weakened by raising the temperature. These samples were subjected to an immersion study. Three samples were immersed in three solutions each. The metal pieces were dipped in 100 mL of 1 M HCl acid solution for 48 hours along with 500 mg of each inhibitor. The prepared compound's corrosion-related structural properties were calculated using a Marvin sketch. The outcomes were correlated with the corrosion study [29].

Theoretical study on molecular structures

The prepared compound's corrosion-related structural properties were calculated using a Marvin sketch. Using the software, pH versus charge graph and Morgan donor-acceptor nature with respect of charges has plotted using the updated structure. The outcomes were correlated with the corrosion study [30]. A measurement of the inhibition tendency was evaluated under dynamic circumstances and tried to justify the corrosion control of the compounds.

RESULTS AND DISCUSSION

Microstructure analysis

The Table 2 represents the tensile strength of nine samples which have 134.5 MPa and maximum of 475 MPa.

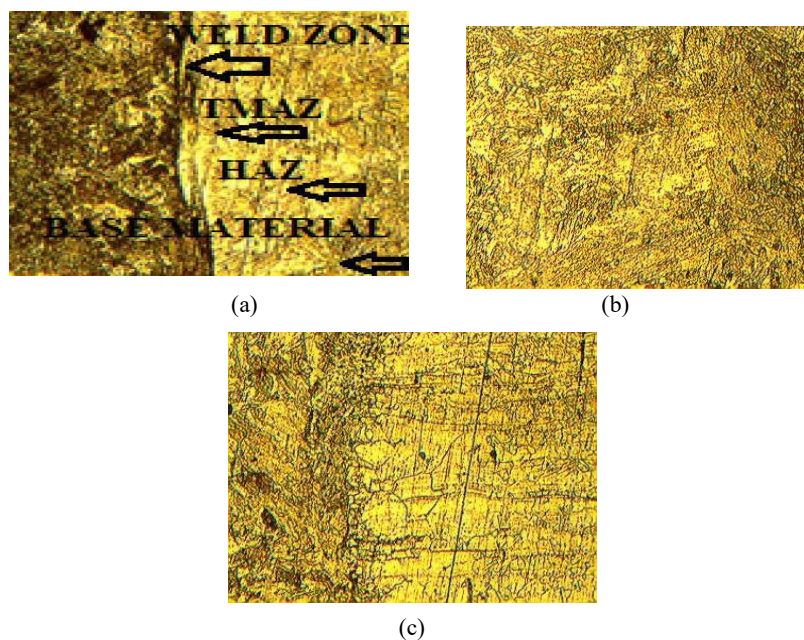


Figure 4. (a, b, c) Microstructure for highest tensile strength sample in a different zone.

Figure (4a) shows the pulsed fiber laser welded zone at the right side AISI 316 with dendritic grains of austenite of the filler material. Figure (4b) shows the parent metal AISI316 microstructure with fine austenite grains. The AISI316 side shows the fusion is effective and complete. Grain growth is observed at the fusion zone of the AISI 316L. Figure (4c) shows the interface zone of the AISI 410 with fine martensite due to weld heat. The maximum tensile strength is due to the maximum amount of metal flow across the weld zone in which the defects are minimal. Dendrite formation and fine martensite formation also contribute to this high strength.

The sample's corrosion-protective nature was investigated by the weight loss method. Three isatin-based Schiff bases were used for the inhibition study in acid solution. Initially, the rectangle coupons were prepared for weight loss study. Figure 5 a, b, c shows the test samples immersed in a corrosive medium and samples after the corrosion test.

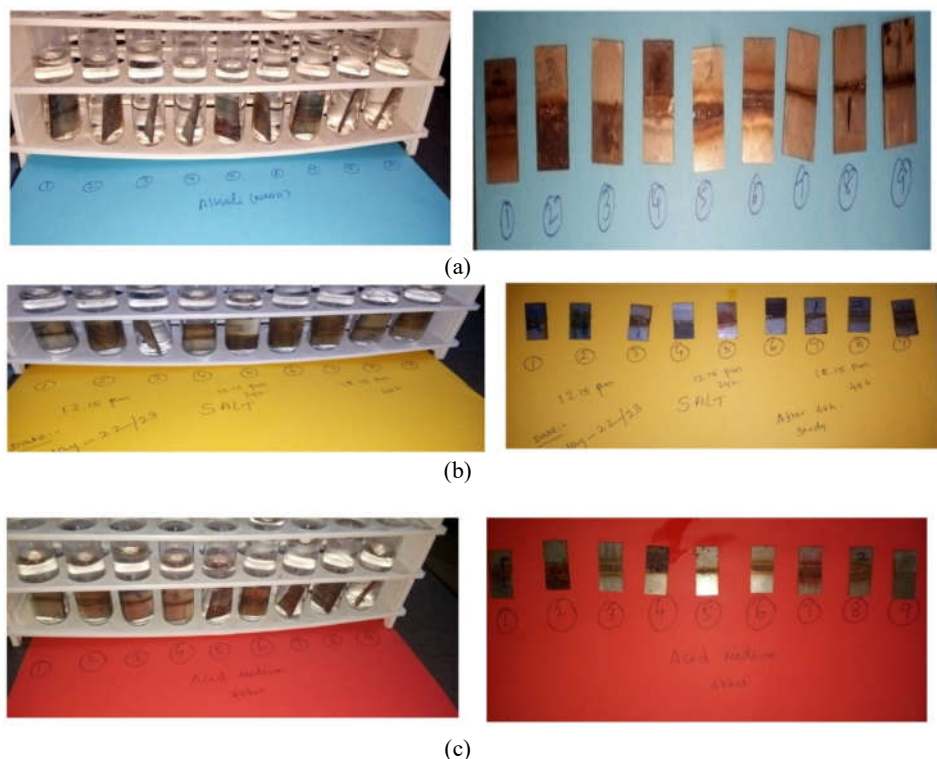


Figure 5. (a, b, c) samples immersed in three different solutions.

Samples are carefully weighed in a PCE-DMS 200 laboratory balance to measure the weight loss in grams due to corrosion. The 1 M artificial salt solution was prepared using ordinary impure salt crystals with a pH of 7.7. The weight of the 9 samples was calculated and it was immersed in the artificial salt solution for 48 hours. The weights of the corroded samples were weighed before and after drying were recorded. The measured weight and weight loss of the samples along with the pH are displayed in Table 3(a). It was figured out that the samples' weight loss had increased and decreased. The maximum weight loss was reported in sample 1 and it was

0.026 g weight. Alahiane *et al.* [31] suggested that the presence of chloride ions [Cl⁻] contributed to allowing [Cl⁻] to interact with the surface of the steel specimen by dissolving the steel's passive layer. The results demonstrated the importance of initiating active corrosion reactions. Sample 2 shows no weight loss which indicates that there is no corrosion. The amount of weight lost in sample 6 is 0.001 g, which is very low and it shows that there is very little corrosion in the sample.

Table 3. (a) Recorded weight loss in salt medium.

Test sample	Initial weight [g]	Before dry weight [g]	After well dried [g]	Weight loss [g]	pH
1	9.51	9.489	9.484	0.026	7.7
2	9.585	9.574	9.585	0.00	7.7
3	6.403	6.395	6.397	0.006	7.7
4	6.441	6.432	6.439	0.002	7.7
5	6.922	6.912	6.910	0.012	7.7
6	9.584	9.574	9.574	0.001	7.7
7	9.601	9.593	9.593	0.013	7.7
8	6.886	6.877	6.877	0.009	7.7
9	9.604	9.596	9.596	0.008	7.7

The acid solution selected is 1 M HCl with a pH of 0.13. The weight of the 9 samples was calculated and it was immersed in the artificial acid solution for 48 hours. The weight of the corroded samples was weighed before and after drying were recorded. The measured weight and weight loss of the samples along with the pH are displayed in below Table 3 (b).

Table 3. (b) Recorded weight loss in acidic medium.

Test sample	Initial weight [g]	Before dry weight [g]	After well dried [g]	Weight loss [g]	pH
1	9.324	9.503	9.318	0.006	0.13
2	9.592	9.890	9.591	0.001	0.13
3	6.505	6.705	6.497	0.008	0.13
4	6.563	6.728	6.559	0.004	0.13
5	6.714	6.835	6.686	0.028	0.13
6	9.353	9.579	9.340	0.013	0.13
7	9.322	9.565	9.315	0.007	0.13
8	6.614	6.812	6.605	0.009	0.13
9	9.306	9.572	9.288	0.018	0.13

The maximum weight loss was reported for sample 7 having lost 0.008 g of weight and sample 4 was reported to have minimum weight loss with 0.003 g lost. Apart from this, samples 6 and 9 have a moderate amount of weight loss. The 1 M sodium hydroxide solution is taken as an acid medium with a pH of 12.96. The weight of the 9 samples was measured at the beginning of the test. The table of observations before the test is given in Table 3(c). The table lists the ranges of parameters used in laser welding, and the initial weight of the samples before testing is weighed and recorded.

The maximum weight loss was reported for sample 7 having lost 0.008 g of weight and samples 1, 4, 5, and 8 reportedly had the minimum amount of loss weight, which is 0.008 g. Tjahjanti *et al.* [32] indicated that the corrosion in NaOH, which is alkaline the environment oxygen species, creates a delay in the corrosion process in the alkaline environment and it was observed the same in the case of fiber laser welded joints. Haewon Byeon *et al.* [33] creates innovative and efficient techniques to prevent corrosion and protect materials in the food,

automotive, and large-scale energy sectors. Neela Murali *et al.* [34] revealed the inhibition of magnesium coated by CeO and ZrO particles. Out of three corrosion mediums, the acid medium exposed the highest weight loss. Hence, this work initiated to propose the control method for the welded joints using organic solid inhibitors. We prepared the isatin-based Schiff bases using heterocyclic ring anisidine. Three Schiff bases ortho-is-sb, meta-is-sb, and para-is-sb were prepared and recrystallized in a 1:1 [ethanol and water] solvent system. The compounds were characterized by ¹H-NMR in a deuterated DMSO solvent. Well-known imine [=C=N-] functional group formed in condensation reaction and observed the absence of anisidine amine hydrogens. From the spectrum, the stable heterocyclic lactam ring proton [-CONH-] peak was observed at 10.1 ppm and confirmed by ¹H-NMR. Aromatic ring protons were detected between 6.4 ppm and 8.5 ppm, which are in concordance with the values reported in previous literature. Nearly at 4.09 ppm, methoxy group (ether) protons were found and confirmed the free ether-linked moiety which can be a donor in the corrosion control study. The prepared isatin Schiff bases have been confirmed by the proton NMR and carried out for the inhibition trials. All are showing 12 protons and confirmed the prepared inhibitor structures and coincidence with the reported values. These compounds were carried for the inhibition study due to more donor functional groups which can push the metal surface electrons towards the metal and control the corrosion in liquid or air medium which is considered as one good inhibitor. Also, it can be understood that, as the peak intensity increases, the amount of hydrogen increases. After the structural confirmation, the compounds were carried out for corrosion inhibition study. The recrystallized compounds were carried out for inhibition study in the acid medium using selected welded samples to know the requirement of the inhibitor in working conditions. The three compounds were tested in 1 M HCl of pH 0.13. The weight loss outcomes were given in Table 4.

Table 3. (c) Recorded weight loss in alkali medium.

Test sample	Initial weight [g]	Before dry weight [g]	After well dried [g]	Weight loss [g]	pH
1	9.491	9.490	9.488	0.003	12.96
2	9.571	9.570	9.567	0.004	12.96
3	6.652	6.65	6.648	0.004	12.96
4	7.024	7.023	7.021	0.003	12.96
5	6.397	6.392	6.394	0.003	12.96
6	9.596	9.595	9.599	0.007	12.96
7	9.480	9.474	9.472	0.008	12.96
8	6.377	6.374	6.374	0.003	12.96
9	9.556	9.553	9.552	0.004	12.96

Table 4. Ortho, meta, and para compounds inhibition weight loss in acidic medium.

Test sample	Initial weight [g]	After well dried [g]	Inhibitor	pH	Weight loss [g]	Mean ± SD
1	9.318	9.317	ortho-is-sb	0.13	0.001	0.0016±0.002
2	9.591	9.591		0.13	Nil	
3	6.497	6.493		0.13	0.004	
4	6.559	6.546	meta-is-sb	0.13	0.013	0.0067±0.007
5	6.686	6.681		0.13	0.005	
6	9.340	9.338		0.13	0.002	
7	9.315	9.315	para-is-sb	0.13	Nil	0.0006 ±0.001
8	6.605	6.603		0.13	0.002	
9	9.288	9.288		0.13	Nil	

Table 4 shows that the amount of corrosion was significantly reduced in the presence of inhibitors. This may be due to the donor character of isatin Schiff base. Based on the above details, the maximum amount of weight loss was recorded in met-isaani hence it is observed to be the weakest inhibitor compound among the three. Whereas weight loss is minimal in or-island and pa-isaani compounds, hence, they may be the best inhibitors among the three. This work extended to define the experimental outcomes of the inhibitor using theoretical structural description. Using Marvin sketch software, this work obtained the isoelectric point, pH vs. charge graph, and Morgan graph to correlate the inhibition nature. The theoretical outcomes showed the isoelectric point for ortho-is-sb [0], meta-is-sb [4.36] and para-is-sb [4.79]. Similarly, Figure 6 indicates that at the corresponding pH values, the compounds do not carry any charges and they remain neutral. At these points, the compounds remain insoluble. At greater negative charges, the compounds show a higher corrosion inhibition rate as per the sacrificial anodic concept. These images show the tendency of molecules to donate and accept hydrogen ions. If it is donating means that electrons are pushed back to the metal surface, so metals will be protected. Suppose if they accept electrons, then they will be subjected to corrosion. Here, the donating tendency is very high for ortho compounds. Also, for meta and para, it is of moderate value. Both iso-electronic and Morgan outcomes have supported the inhibition tendency of the compounds.

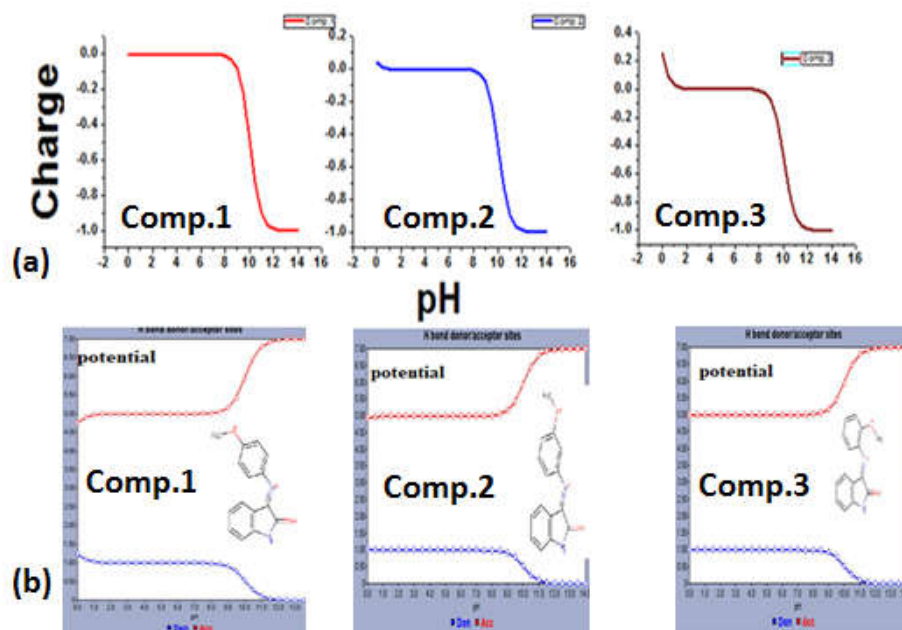


Figure 6. (a) Charge vs pH curves and (b) Morgan - Donor and acceptor graph.

CONCLUSIONS

Fiber laser welding was used to produce a very strong welded joint on AISI 410 and AISI 316 stainless steels. A total of nine samples were welded by varying the process parameters of frequency in the range of 4000-5000 Hz, welding power in the range of 1000-1980 W, and

traverse speed in the range of 3 to 9 mm/min. The corrosion study establishes a high corrosion resistance for AISI 410 and AISI 316L stainless steel. Samples were tested for corrosion resistance in three media. The three media chosen are hydrochloric acid, sodium chloride solution, and sodium hydroxide solution. Three corrosion inhibitors were prepared to study the corrosion resistance of the welded joints. This work can be concluded with the results obtained on the investigation carried out: (i) The AISI 410 and AISI 316L stainless steels are welded with fiber laser welding. (ii) The maximum and minimum tensile strength of the joint is observed as 475.39 MPa, 134.5 MPa, respectively. (iii) Dendrite formation and fine martensite formation also contributes to this high strength. (iv) The corrosion test was carried out in three media: acid, salt, and base. Out of all these tests, the maximum corrosion was found to be in an acidic medium. Similarly, the 5th sample showed maximum weight loss, and sample 2 in salt medium with no weight loss. (v) The three corrosion inhibitors prepared are ortho-is-sb, meta-is-sb and para-is-sb. These were used in acidic media, and the best inhibitor was found to be ortho-is-sb when compared to the other two inhibitors. (vi) The prepared three corrosion inhibitors are ortho-is-sb, meta-is-sb and para-is-sb. These were used in acidic media, and the best inhibitor was found to be para-is-sb (2.7 times greater than ortho and 11.2 times greater than meta-is-sb). (vii) In future, these compounds will be added with organic coating materials and welded joints corrosion resistivity will be investigated.

ACKNOWLEDGEMENT

The compound preparation was monitored by Dr. R. Jayaprakash, Associate Professor at the School of Arts and Science, AV Campus, Paiyanoor, and the authors are grateful for his assistance.

REFERENCES

1. Maurya, A.K.; Pandey, C.; Chhibber, R. Dissimilar welding of duplex stainless steel with Ni alloys: A review. *Int. J. Press. Vessels Pip.* **2021**, *192*, 104439.
2. Srinivasan, P.B.; Muthupandi, V.; Dietzel, W.; Sivan, V. An assessment of impact strength and corrosion behavior of shielded metal arc welded dissimilar weldments between UNS 31803 and IS 2062 steels. *Mater. Des.* **2006**, *27*, 182–191.
3. Hu, Y.; Wu, L.; Zhou, P.; Ye, Y.; Wang, B. Fiber laser welding of Ti–6Al–4V to Inconel 718 bimetallic structure via Cu/Ta multi-interlayer. *Vacuum.* **2021**, *192*, 110461.
4. Geng, Y.; Akbari, M.; Karimipour, A.; Karimi, A.; Soleimani, A.; Afrand, M. Effects of the laser parameters on the mechanical properties and microstructure of weld joint in dissimilar pulsed laser welding of AISI 304 and AISI 420. *Infrared Phys. Technol.* **2019**, *103*, 103081.
5. Ai, Y.; Shao, X.; Jiang, P.; Li, P.; Liu, Y.; Liu, W. Welded joints integrity analysis and optimization for fiber laser welding of dissimilar materials. *Opt. Lasers Eng.* **2016**, *86*, 62–74.
6. Meng, W.; Xu, Z.; Ma, Q.; Yin, X.; Fang, J. Pulse fiber laser welding of AISI 321-AISI 405 stainless steel thick plates butt joints. *J. Mater. Process. Technol.* **2019**, *271*, 214–225.
7. Mosavi, A.; Soleimani, A.; Karimi, A.; Akbari, M.; Karimipour, A.; Karimipour, A. Investigating the effect of process parameters on the mechanical properties and temperature distribution in fiber laser welding of AISI304 and AISI 420 sheets using response surface methodology. *Infrared Phys. Technol.* **2020**, *111*, 103478.
8. Sun, Y.; Wu, L.; Tan, C.; Zhou, W.; Chen, B.; Song, X.; Zhao, H.; Feng, J. Influence of Al-Si coating on microstructure and mechanical properties of fiber laser welded 22MnB5 steel. *Opt. Laser Technol.* **2019**, *116*, 117–127.

9. Zhang, D.; Wang, M.; Shu, C.; Zhang, Y.; Wu, D.; Ye, Y. Dynamic keyhole behavior and keyhole instability in high power fiber laser welding of stainless steel. *Opt. Laser Technol.* **2019**, *114*, 1–9.
10. Cheng, M.; He, P.; Lei, L.; Tan, X.; Wang, X.; Sun, Y.; Li, J.; Jiang, Y. Comparative studies on microstructure evolution and corrosion resistance of 304 and newly developed high Mn and N austenitic stainless steel welded joints. *Corros. Sci.* **2021**, *183*, 109338.
11. Reka Fabian, E.; Kuti, J.; Gati, J.; Toth, L. Corrosion behavior of welded joints in different stainless steels. *Rev. Chim.* **2020**, *71*, 440–449.
12. Verma, J.; Taiwade, R. V. Dissimilar welding behavior of 22% Cr series stainless steel with 316L and its corrosion resistance in a modified aggressive environment. *J. Manuf. Process.* **2016**, *24*, 1–10.
13. Zhang, X.; Mi, G.; Wang, C. Microstructure and performance of hybrid laser-arc welded high-strength low alloy steel and austenitic stainless steel dissimilar joint. *Opt. Laser Technol.* **2020**, *122*, 105078.
14. Kimura, M.; Ohara, K.; Kusaka, M.; Kaizu, K.; Hayashida, K. Effects of tensile strength on friction welding condition and weld faying surface properties of friction welded joints between pure copper and austenitic stainless steel. *J. Adv. Join. Process.* **2020**, *2*, 100028.
15. Poo-arporn, Y.; Duangnil, S.; Bamrungkoh, D.; Klangkaew, P.; Huasranoi, C.; Pruekthaisong, P.; Boonsuya, S.; Chairapa, J.; Ruangvittayanon, A.; Saisombat, C. Gas tungsten arc welding of copper to stainless steel for ultra-high vacuum applications. *J. Mater. Process. Technol.* **2020**, *277*, 116490.
16. Chen, S.; Huang, J.; Xia, J.; Zhao, X.; Lin, S. Influence of processing parameters on the characteristics of stainless steel/copper laser welding. *J. Mater. Process. Technol.* **2015**, *222*, 43–51.
17. Cheng, Z.; Liu, H.; Huang, J.; Ye, Z.; Yang, J.; Chen, S. MIG-TIG double-sided arc welding of copper-stainless steel using different filler metals. *J. Manuf. Process.* **2020**, *55*, 208–219.
18. Sathish, R.; Rao, V. S. Corrosion studies on friction welded dissimilar aluminum alloys of AA7075-T6 and AA6061-T6. *Int. J. Electrochem. Sci.* **2014**, *9*, 4104–4113.
19. Alahiane, M.; Oukhrib, R.; Albrimi, Y. A.; Oualid, H. A.; Bourzi, H.; Akbour, R. A.; Assabbane, A.; Nahle, A.; Hamdani, M. Experimental and theoretical investigations of benzoic acid derivatives as corrosion inhibitors for AISI 316 stainless steel in hydrochloric acid medium: DFT and Monte Carlo simulations on the Fe [110] surface. *RSC Adv.* **2020**, *10*, 41137–41153.
20. Behpour, M.; Ghoreishi, S. M.; Soltani, N.; & Salavati-Niasari, M. The inhibitive effect of some bis-N,S-bidentate Schiff bases on corrosion behavior of 304 stainless steel in hydrochloric acid solution. *Corros. Sci.* **2009**, *51*, 1073–1082.
21. Gnanavelbabu, A.; Prahadeeswaran, M.; Rai, R.; Ross, N. S.; Gupta, M. K. Tribo-corrosive wear behaviour of squeeze-casted Mg/TiN/hBN composite under different ageing temperature. *Tribol. Int.* **2023**, *187*, 108748.
22. Gnanavelbabu, A.; Vinothkumar, E.; Ross, N.S.; Kuntoglu, M. Investigating the influence of NaCl concentration on the electrochemical corrosion behavior of metal oxide reinforced magnesium matrix composites. *Archiv. Civ. Mech. Eng.* **2023**, *23*, 113.
23. Gnanavelbabu, A.; Vinothkumar, E.; Ross, N. S.; Gupta, M. K.; Jamil, M. Tribo-corrosive wear and mechanical properties of nanoparticles reinforced Mg-AZ91D composites, *Tribol. Int.* **2023**, *178*, 108054.
24. Ayyadurai, G. K.; Jayaprakash, R.; Rathika, S. Theoretical Molecular Properties Prediction, Docking and Antimicrobial Studies on Anisidine-Isatin Schiff Bases, *Asian J. Chem.* **2021**, *3*, 3025–3030.
25. Al-Amiery, A.A.; Al-Azzawi, W.K.; Isahak, W.N.R.W. Isatin. Schiff base is an effective corrosion inhibitor for mild steel in hydrochloric acid solution: Gravimetric, electrochemical, and computational investigation. *Sci. Rep.* **2022**, *12*, 17773.

26. Azizian, J.; Mohammadi, M.K.; Firuzi, O.; Razzaghi-asl, N.; Miri, R. Synthesis, biological activity and docking study of some new isatin Schiff base derivatives. *Med. Chem. Res.* **2012**, *21*, 3730–3740.
27. Eugene, U.; Orsquo Donnell, P.S.; Ifeoma, V. J.; Feyisayo, V. A. The effect of corrosion inhibitors on stainless steels and aluminium alloys: A review. *Afr. J. Pure Appl. Chem.* **2016**, *10*, 23–32.
28. Ahmed, M.H.O.; Al-Amiery, A.A.; Al-Majedy, Y.K.; Kadhun, A.A.H.; Mohamad, A.B.; Gaaz, T.S. Synthesis and characterization of a novel organic corrosion inhibitor for mild steel in 1 M hydrochloric acid. *Results Phys.* **2018**, *8*, 728–733.
29. Arrousse, N.; Salim, R.; Kaddouri, Y.; Zahri, D.; El Hajjaji, F.; Touzani, R.; Taleb, M.; Jodeh, S. The inhibition behavior of two pyrimidine-pyrazole derivatives against corrosion in hydrochloric solution: Experimental, surface analysis and in silico approach studies. *Arab. J. Chem.* **2020**, *13*, 5949–5965.
30. De Assis, S.L.; Wolyne, S.; Costa, I. Corrosion characterization of titanium alloys by electrochemical techniques. *Electrochim. Acta* **2006**, *51*, 1815–1819.
31. Alahiane, M.; Oukhrib, R.; Albrimi, Y.A.; Oualid, H.A.; Bourzi, H.; Akbour, R.A.; Assabbane, A.; Nahlé, A.; Hamdani, M. Experimental and theoretical investigations of benzoic acid derivatives as corrosion inhibitors for AISI 316 stainless steel in hydrochloric acid medium: DFT and Monte Carlo simulations on the Fe [110] surface. *RSC Adv.* **2020**, *10*, 41137–41153.
32. Tjahjanti, P.H.; Kurniawan; M.M.; Firdaus, R.; Iswanto; A.T. Experimental study of corrosion rate on st60 steel as a result of immersion in HCl, NaOH, and NaCl solutions. *IOP Conf. Ser.: Mater. Sci. Eng.* **2020**, *725*, 012038.
33. Byeon, H.; Haribabu, K.; Kiradoo, G.; Sreenivasan, V.S.; Sivaprakash, M.; Richard, S.; Sunil, J. Evaluation of the physiochemical and electrochemical behavior of reduced graphene functionalized copper nanostructure as an effective corrosion inhibitor. *Bull. Chem. Soc. Ethiop.* **2024**, *38*, 269–280.
34. Neela Murali, V.K.; Starvin, M.S.; Bensam Raj, J. Exploring the corrosion inhibition of magnesium by coatings formulated with nano CeO and ZrO particles. *Bull. Chem. Soc. Ethiop.* **2023**, *37*, 1299–1306.